

Local Gauge Invariance and Formation of Topological Defects*

Arttu Rajantie

DAMTP, CMS, Wilberforce Road, Cambridge CB3 0WA, United Kingdom

In superconductors, and in other systems with a local $U(1)$ gauge invariance, there are two mechanisms that form topological defects in phase transitions. In addition to the standard Kibble mechanism, thermal fluctuations of the magnetic field also lead to defect formation. This mechanism is specific to local gauge theories, predicts a qualitatively different spatial defect distribution and is the dominant source for topological defects in slow transitions. I review the arguments that lead to these conclusions and discuss possibilities of testing the scenario in superconductor experiments.

PACS numbers: 11.15.Ex, 11.27.+d, 74.40.+k

1. INTRODUCTION

The Kibble mechanism¹ gives a very simple and elegant description for the formation of topological defects in symmetry breaking phase transitions, and has been studied intensively in experiments with liquid crystals² and liquid Helium.^{3,4,5} Even though the results do not agree completely with the theoretical predictions, the mechanism itself is still believed to be correct. Instead, the discrepancies are presumably due to the extra assumptions one has to make about the dynamical time and length scales of the system in order to derive quantitative predictions.^{6,7}

More recently, defect formation has also been studied in superconductors⁸ and Josephson junctions.⁹ These systems differ from liquid Helium in a significant way: the order parameter, i.e., the Cooper pair, is electrically charged, and the symmetry that is broken in the phase transition is the local $U(1)$ gauge invariance associated with electromagnetism. This means that the arguments behind the Kibble mechanism cannot be applied directly, and

*Talk given at the ULTI symposium, Pohja, Finland, 10–14 January 2001.

A. Rajantie

there has been some discussion over the years on how it should be modified.¹⁰

However, it was recently pointed out by myself and Hindmarsh¹¹ that it is not enough to simply modify the Kibble mechanism, because there is another, totally separate effect that leads to defect formation. While the Kibble mechanism is based on the dynamics of the order parameter field, this new scenario relies on thermal fluctuations of the magnetic field. It also leads to predictions that are qualitatively different from those of the Kibble scenario.

Unfortunately, the experimental setup in Ref. 8 was such that the contribution from our mechanism was negligible. Basically, one would have to be able to detect the positions and signs of individual vortices in order to be able to test the mechanism.

The aim of this paper is to review the mechanism of Ref. 11 and to discuss its predictions for a superconducting film.

2. KIBBLE MECHANISM

Let us first review the Kibble mechanism and consider a simple two-dimensional toy model with an U(1) symmetry, i.e., our order parameter ψ is a complex scalar field. The thermodynamics of the model is described by the free energy,¹² which we approximate in the standard way by

$$F[\psi] = \int d^2x \left[\vec{\nabla}\psi^* \cdot \vec{\nabla}\psi + m^2\psi^*\psi + \lambda(\psi^*\psi)^2 \right], \quad (1)$$

where $m^2 \sim T - T_c$.

When the critical temperature is approached from the symmetric phase, the correlation length of the order parameter, i.e., the coherence length ξ , diverges but it cannot grow arbitrarily fast, because at least it is constrained by the speed of light. Therefore, if the phase transition takes place in a finite time, the coherence length reaches a finite maximal value $\hat{\xi}$, and if we divide the system in domains of radius $\hat{\xi}$, the phase angle of the order parameter is uncorrelated between different domains. At points where three or more domains meet, there is a fixed probability that the phase angle cannot be smoothly interpolated between the domains, in which case a vortex is formed. Thus, the number density of vortices must behave as

$$n_{\text{Kibble}} \sim \hat{\xi}^{-2}. \quad (2)$$

Because the mechanism is based on very general assumptions only, this result applies to all systems in which a global U(1) symmetry breaks down

Formation of Topological Defects

spontaneously, for instance to ${}^4\text{He}$. It can also be generalized to other symmetry groups very easily. However, in order to make contact with experiments, one would have to be able to predict the value of $\hat{\xi}$. An upper bound can be obtained from causality,¹ but a more precise estimate requires extra assumptions about the dynamics of the system.^{6,7}

3. GAUGE INVARIANCE

If the order parameter field is electrically charged, as it is, e.g., in the case of superconductors, it couples to the electromagnetic vector potential. Then the analogue of the approximate free energy (1) is¹²

$$F[\psi, \vec{A}] = \int d^2x \left[\frac{1}{2} B^2 + \vec{D}\psi^* \cdot \vec{D}\psi + m^2 \psi^* \psi + \lambda (\psi^* \psi)^2 \right], \quad (3)$$

where B is the magnetic induction,¹ $B = \partial_x A_y - \partial_y A_x$, and \vec{D} is the covariant derivative $\vec{D} = \vec{\nabla} + ie\vec{A}$, and \vec{A} is the electromagnetic vector potential (gauge field).

The coupling to \vec{A} has the important consequence that the U(1) symmetry becomes local; the free energy is invariant under all transformations

$$\psi(\vec{x}) \rightarrow \exp(i\Lambda(\vec{x}))\psi(\vec{x}), \quad \vec{A}(\vec{x}) \rightarrow \vec{A}(\vec{x}) - \frac{i}{e} \vec{\nabla} \Lambda(\vec{x}), \quad (4)$$

where $\Lambda(\vec{x})$ can be any real function of \vec{x} .

In particular, this local gauge invariance means that the phase angle of ψ does not have any physical meaning, because it can always be transformed away by a suitable choice of Λ . For this reason, one cannot talk about domains of correlated ψ anymore. In the global case, the gradient term in the free energy (1) tends to make the order parameter aligned, but in the local case, it is the covariant derivative $\vec{D}\psi$ and not the gradient that will be minimized. In the special case in which $\vec{A} = 0$, there is no difference, but in practice there are always non-zero thermal fluctuations present in the \vec{A} field. If \vec{A} is non-zero, the covariant derivatives cannot typically be minimized everywhere at the same time, and this leads to vortex formation.

In fact, this effect can easily be seen in simple cases in which the initial value of the vector potential \vec{A} has been set by hand. As a very simple example, let us think of a phase transition in the presence of an homogeneous magnetic field $B(\vec{x}) = B_0$. When the system enters the broken phase, the dynamics tries to minimize $\vec{D}\psi$. Let us write $\psi(\vec{x}) = v(\vec{x}) \exp(i\theta(\vec{x}))$, and

¹In three dimensions, B would, of course, be a vector field $\vec{B} = \vec{\nabla} \times \vec{A}$.

A. Rajantie

consider a circular curve of radius R . At every point on this curve, the system tries to minimize the covariant derivative, but that leads to the result

$$\int_C d\vec{x} \cdot \vec{\nabla} \theta = \frac{1}{e} \int_C d\vec{x} \cdot \vec{A} = \frac{1}{e} \int_S d^2x B = \frac{2\pi R B_0}{e}. \quad (5)$$

This means that if $R B_0 \gtrsim e$, non-zero winding number is preferred, and consequently a vortex is formed. This formation of an Abrikosov vortex lattice is a well-known phenomenon in superconductor physics.

4. PLANE WAVE

In order to understand the dynamics of phase transitions in which the magnetic field is inhomogeneous, it is instructive to consider first a plane wave. Let us assume that there is a standing electromagnetic wave trapped inside our two-dimensional system,

$$B(x, y) = B_0 \sin(kx), \quad (6)$$

where k is the wave number of the wave.

The free energy (3) by itself determines only the thermodynamics of the model, not the dynamics. For that, we need the equations of motion, and here we will consider a simple, “relativistic” model,

$$\begin{aligned} \partial_0^2 \psi &= \vec{D}^2 \psi - V'(\psi), \\ \partial_0 E_i &= \epsilon_{ij} \partial_j B + 2e \text{Im} \psi^* D_i \psi, \\ \vec{\nabla} \cdot \vec{E} &= 2e \text{Im} \psi^* \partial_0 \psi, \end{aligned} \quad (7)$$

where $V(\psi) = m^2 |\psi|^2 + \lambda |\psi|^4$. Note that there is no external magnetic field acting on the system; instead, Eq. (6) merely specifies the initial conditions for the time evolution.

Let us now “quench” the system into the broken phase by changing m^2 rapidly. To be specific, let us assume that

$$m^2(t) = -m_0^2 \frac{t}{\tau_Q}. \quad (8)$$

If τ_Q is small enough in comparison to the wave number k , the situation in the regions in which B is, say, positive looks exactly the same as in the case of a homogeneous magnetic field. Therefore, vortices with a positive sign will form. Likewise, in the regions with negative B , vortices with a negative sign form. Fig. 1 shows the configuration of the B field at different times during such a transition. In the initial state, the order parameter field ψ was given

Formation of Topological Defects

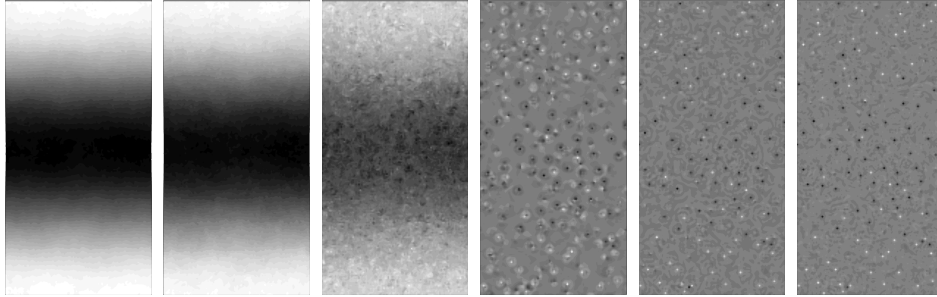


Fig. 1. The time evolution of the local magnetic induction $B(\vec{x})$ in a slow phase transition, starting from a plane wave configuration. Shades from white to black indicate field values from positive to negative. Initially, the amplitude of the field is very small, but the contrast of the plot is adjusted accordingly to make it visible. In the final state, the flux is confined into vortices inside which the value of $B(\vec{x})$ is very high. The signs of the vortices are strongly correlated with the initial value of B at each point.

tiny random fluctuations, and then the mass parameter was decreased so that the system underwent a phase transition to the broken phase. The plot shows clearly how the signs of the vortices are correlated with the initial value of the magnetic induction at each point. Note, however, that the agreement is not perfect. These vortices with “wrong” signs are formed by the Kibble mechanism.

On the other hand, if τ_Q is large enough, the transition is adiabatic. The amplitude of B decreases, and the system ends up in the equilibrium state, which contains no vortices because of the absence of any external magnetic fields. This shows that for each k there is a critical value of τ_Q so that if the transition is faster, vortices will form. We can also invert this relation and define for each τ_Q a critical wavenumber $\hat{k}(\tau_Q)$.

5. THERMAL EQUILIBRIUM

In practice, we are not interested in creating vortices by external magnetic fields or by standing electromagnetic waves. Instead, we would like to understand what happens when the transition starts from thermal equilibrium. However, similar arguments apply to that case as well, because thermal fluctuations alone can act as seeds for vortex formation.

In thermal equilibrium, the state of the system is not described by a single field configuration, but by an ensemble of configurations in which the probability of any given configuration is proportional to $\exp(-E[\psi, \vec{A}]/T)$.

A. Rajantie

Here $E[\psi, \vec{A}]$ is the energy of the field configuration, and is essentially equal to the free energy (3). Because of the smallness of the gauge coupling constant e , we can neglect the coupling to ψ and approximate the energy by

$$E[\vec{A}] \approx \int d^2x \frac{1}{2} B(\vec{x})^2. \quad (9)$$

Thus the probability distribution of B is almost Gaussian, and the field strength is totally uncorrelated between all the points in the coordinate space. If we write the energy in the Fourier space, we find that the same is true there as well,

$$E[\vec{A}] \approx \int \frac{d^2k}{(2\pi)^2} \frac{1}{2} |B(\vec{k})|^2, \quad (10)$$

i.e., the amplitude of each Fourier mode independent of all the others and has a Gaussian distribution with a k -independent width. As long as the system is in the symmetric phase, each mode also behaves dynamically independently of the other modes. Therefore we can estimate that in a transition with quench time τ_Q , the modes with $|\vec{k}| \lesssim \hat{k}(\tau_Q)$ equilibrate, but the modes with $|\vec{k}| \gtrsim \hat{k}(\tau_Q)$ fall out of equilibrium and their distribution remains the same as it was in the symmetric phase before the transition.

To make comparison with the Kibble mechanism easier, we denote the wavelength corresponding to \hat{k} by $\hat{\xi} = 2\pi/\hat{k}$. The above implies that if we concentrate on a region S of radius $\hat{\xi}$, the total magnetic flux through this region does not change significantly in the transition. Inside the region, the flux rearranges itself in order to minimize the energy, i.e., it forms a vortex “lattice” in which all the vortices have equal sign. Therefore, we can estimate the number of vortices in the region S after the transition by calculating the typical flux through it at the time of the transition, and this is approximately the same as it is in the symmetric phase. Because of the Gaussianity of the probability distribution, it is easy to calculate,

$$\left(\Phi_S^{\text{typ}}\right)^2 \approx \langle \Phi_S^2 \rangle = \int d^2x d^2x' \langle B(\vec{x}) B(\vec{x}') \rangle = \int d^2x T = \pi \hat{\xi}^2 T. \quad (11)$$

Therefore, the typical number of vortices through the region S in the broken phase is

$$N_S = \Phi_S^{\text{typ}} / \Phi_0 \approx \frac{e}{2\pi} T^{1/2} \hat{\xi}, \quad (12)$$

and, consequently, the number density of vortices is

$$n \approx \frac{N_S}{\pi \hat{\xi}^2} \approx \frac{e}{2\pi} T^{1/2} \hat{\xi}^{-1}. \quad (13)$$

Note that this estimate was for a two-dimensional system, and therefore e is not a dimensionless number like it is in three dimensions, but instead,

Formation of Topological Defects

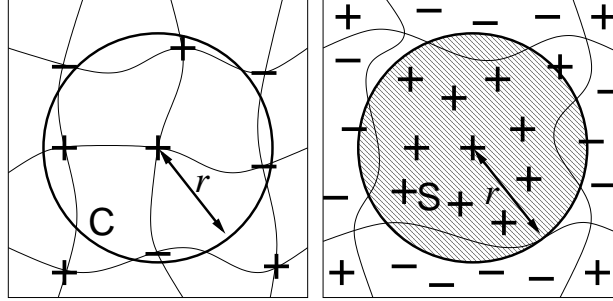


Fig. 2. The winding number of a circular curve of radius r centred at a positive vortex, $N_C(r)$, behaves differently in the Kibble mechanism (left) and in the local gauge theory (right).

it has a dimension of energy^{1/2}. The three-dimensional case has also some other differences, and it will be discussed in Section 7.

The essential point in Eq. (13) is the relation $n \propto \hat{\xi}^{-1}$, which differs from the prediction of the Kibble mechanism $n \propto \hat{\xi}^{-2}$ in Eq. (2). In order to really predict the vortex number density in either case, we must be able to calculate $\hat{\xi}$ and that depends sensitively on the dynamics of the system. However, if we assume that the critical wavelength $\hat{\xi}$ is or the same order of magnitude in both cases, Eq. (13) becomes greater than Eq. (2) when $\hat{\xi} \gtrsim 2\pi/eT^{1/2}$. Because long wavelengths correspond to slow transitions, we can conclude that this mechanism dominates in slow transitions.

6. SPATIAL DISTRIBUTION

Even without any assumption on $\hat{\xi}$, our mechanism can be tested by studying the spatial distribution of vortices. One particularly simple way of seeing this is by considering the average winding number along a circular curve of radius r centred at a vortex of positive sign (see Fig. 2). In practice, we pick a vortex, draw a circle of radius r around it and count the number of vortices of the same sign as the one at the centre minus the number of vortices of opposite sign, and average this over all vortices. We denote this quantity by $N_C(r)$. Obviously, $N_C(0) = 1$, because then only the vortex itself is counted.

Let us first consider the Kibble mechanism. In this case, the vortex number is determined by the phase angle $\gamma = \arg \psi$ of the order parameter field, and we can write

$$N_C(r) = \int_C d\vec{r} \cdot \vec{\nabla} \gamma. \quad (14)$$

A. Rajantie

The vortices are formed at the points where domains meet, and therefore the distance to the nearest vortex is roughly the domain size $\hat{\xi}$. Therefore, as long as $r \ll \hat{\xi}$, $N_C(r)$ does not change significantly as we increase r .

However, when $r \gg \hat{\xi}$, every point on the curve C is uncorrelated with the centre of the curve, because the correlation length $\hat{\xi}$ is less than r . Therefore the integral (14) must be independent of whether there is a positive or a negative vortex at the centre. This implies that it cannot have a preferred sign, and therefore it must vanish on average. Summarizing, we find that in the Kibble mechanism

$$N_C(r) \approx \begin{cases} 1, & r \lesssim \hat{\xi}, \\ 0, & r \gtrsim \hat{\xi}. \end{cases} \quad (15)$$

In our mechanism, the vortex number is determined by the magnetic field, and therefore it is more convenient to write²

$$N_C(r) = \int_{S(C)} d^2x B(\vec{x}), \quad (16)$$

where $S(C)$ is the region bounded by the curve C . In this case, the vortices are inside domains and all the vortices in a given domain have equal sign. When we start increasing r from zero, each new vortex we pick up has the same sign as the one at the origin, as long as $r \ll \hat{\xi}$. This implies that $N_C(r)$ increases with increasing r . However, when $r \gg \hat{\xi}$, the sign of any new vortex encountered is independent of the vortex at the centre, and therefore, on average, $N_C(r)$ remains constant. Thus we conclude that

$$N_C(r) \approx \begin{cases} 1 + cr^2, & r \lesssim \hat{\xi}, \\ \text{constant } (\geq 1), & r \gtrsim \hat{\xi}, \end{cases} \quad (17)$$

where c is some constant.

The two predictions (15) and (17) are qualitatively different, and therefore it is easy to determine which of the mechanisms dominates if one is able to measure the spatial distribution of vortices in the final state. In numerical simulations, this is straightforward, and we have carried out this measurement.¹¹

In our simulations, we used a thin ($120 \times 120 \times 5$) three-dimensional lattice, and solved numerically the equations of motion

$$\begin{aligned} \partial_0^2 \psi &= \vec{D}^2 \psi - V'(\psi), \\ \partial_0 \vec{E} &= \vec{\nabla} \times \vec{B} + 2e \text{Im} \psi^* \vec{D} \psi, \\ \vec{\nabla} \cdot \vec{E} &= 2e \text{Im} \psi^* \partial_0 \psi. \end{aligned} \quad (18)$$

² In a suitably chosen gauge, Eq. (14) is valid in the gauge theory as well, but the arguments that lead to the prediction (15) are not.

Formation of Topological Defects

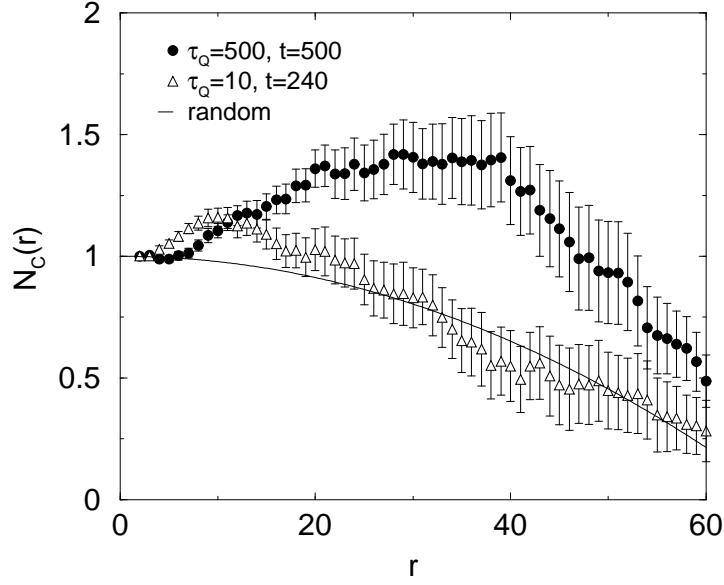


Fig. 3. The average of $N_C(r)$ as a function of r after slow ($\tau_Q = 500$) and fast ($\tau_Q = 10$) transitions (from Ref. 11). The solid line is a benchmark curve, which shows the behaviour in the case where there are no correlations at all between vortices. In both cases the data points are significantly above this curve at short distances, which indicates positive correlations at short distances, just like predicted by Eq. (17). The signal gets stronger in slow transitions.

The time step was $\delta t = 0.05$ in units where the lattice spacing is one. The coupling constants were $e = 0.3$ and $\lambda = 0.18$. Because $\lambda > e^2$, this corresponds to a type-II superconductor. We first thermalized the system to temperature $T = 6$ in the symmetric phase using a hybrid Monte Carlo algorithm. Then, we evolved the system according to the equations of motion (18), changing the mass term as

$$m^2(t) = m_0^2 - \delta m^2 \left(\frac{4}{3\pi} \arctan \frac{t}{\tau_Q} + \frac{1}{3} \right). \quad (19)$$

Here $m_0^2 = 1.4$ is the initial value at $t = -\tau_Q$ when the quench begins and $\delta m^2 = 3.2$ was chosen in such a way that the transition takes place at $t \approx 0$. In the final state, we measured the function $N_C(r)$ and averaged it over several initial configurations taken from the thermal ensemble. The results are shown in Fig. 3 for two different quench rates. The solid line in the plot is to illustrate the effects of the finite system size. Because the total flux

A. Rajantie

through the system is fixed to zero by the boundary conditions, $N_C(r)$ would not be unity even for a random distribution of vortices. Instead, it would decrease as $N_C(r) = 1 - \pi r^2/A$, where $A = 120^2$ is the cross-sectional area of the lattice. This is shown as the solid curve in Fig. 3. The fact that the data points are significantly above it indicates that the vortex distribution indeed behaves as in Eq. (17), supporting our mechanism.

7. THREE DIMENSIONS

A superconductor film resembles in many respects the thin three-dimensional model discussed in the previous section, and therefore it might seem that the result would apply directly to a real experimental situation. However, there is an important difference: In reality the magnetic field lives in three dimensions, and the part of it that is outside the superconductor also contributes to the free energy.

For simplicity, we shall now assume that in the symmetric phase, the magnetic field behaves as if it was in vacuum. This is not a totally unreasonable approximation, because if the superconducting film is thin, the energy of a typical field configuration is dominated by the contribution from the vacuum outside the film.

Furthermore, we assume that when the film becomes superconducting, it starts to dominate the dynamics of the magnetic field. Essentially this means that we can treat the vortices, instead of the magnetic field, as the relevant degrees of freedom.

Again, we have to estimate the typical flux through a circular loop of radius $\hat{\xi}$ on the film. The configuration of minimal energy in which the flux is Φ , is simply the magnetic dipole, and its energy is roughly

$$E(\Phi, \hat{\xi}) \sim \frac{\Phi^2}{\mu_0 \hat{\xi}}. \quad (20)$$

We can estimate that thermal fluctuations can generate this configuration if its energy is less than the temperature, $E \lesssim k_B T$. This reasoning leads to

$$\Phi \sim \sqrt{\mu_0 k_B T \hat{\xi}} = \frac{e}{\pi \hbar} \left(\mu_0 k_B T \hat{\xi} \right)^{1/2} \times \Phi_0. \quad (21)$$

Dividing this by the area of the loop, we find the number density

$$n \sim \frac{e}{\pi \hbar} \left(\frac{\mu_0 k_B T}{\hat{\xi}^3} \right)^{1/2}. \quad (22)$$

Formation of Topological Defects

It is more difficult to estimate $\hat{\xi}$, because it depends on the dynamical properties of the superconductor near the transition point, and we don't attempt to do that here. Instead, we calculate how large $\hat{\xi}$ must be in a realistic experiment so that the correlations between vortices would be clear enough to be observed. This requires that the number of vortices inside each domain is much greater than one, i.e.,

$$N_S \approx \frac{e}{\pi\hbar} \left(\mu_0 k_B T \hat{\xi} \right)^{1/2} \gg 1. \quad (23)$$

The critical temperature of, e.g., YBCO superconductors is $T = 90$ K, and this leads to the estimate

$$\hat{\xi} \gg \frac{\pi^2 \hbar^2}{e^2 \mu_0 k_B T} \approx 3 \text{ mm}, \quad (24)$$

which is a very reasonable size from the experimental point of view.

Experiments like this have not been carried out yet, and there may well be technical difficulties involved in the measurement of the spatial distribution of the vortices after the transition. In particular, one will have to be able to freeze the locations of the vortices so that they don't annihilate before the measurement has been finished.

On the other hand, an otherwise very similar experiment has been carried out recently by Carmi et al.⁸ Instead of measuring the number and locations of individual vortices, they measured the total net flux, i.e., the number of positive vortices minus the number of negative vortices. The result they found was that the flux was consistent with zero, which contradicts the predictions of the Kibble mechanism. The mechanism presented in this paper cannot explain this result, because it would typically predict an extra set of vortices in addition to those formed by the Kibble mechanism. It does not make the discrepancy with the experiment any worse either, because our mechanism does not actually change the total flux through the film at all, and therefore the variation in the total net flux in the final state is simply equal to the variation in the initial flux, i.e., very small.

8. CONCLUSIONS

I have discussed the scenario of defect formation presented in Ref. 11 from the point of view of superconductors. This scenario is not merely a modification to the standard Kibble mechanism, but a totally separate mechanism, and in a general phase transition, both of them form vortices. Which one of them dominates, depends on the details of the transition.

A. Rajantie

Although estimating the density of vortices formed in the transition by either mechanism requires a detailed knowledge about the dynamics of the system, it is possible to derive simple and robust predictions for the spatial distribution of vortices. Basically, the Kibble mechanism predicts negative correlations between vortices, i.e., that nearby vortices have opposite signs, whereas the mechanism discussed here predicts positive correlations. These predictions can be tested experimentally, if it is possible to measure the locations and signs of individual vortices after the phase transition. The domain size needed for these vortex-vortex correlations to be significant in YBCO superconductors, being of the order of centimeter, is suitable for experiments.

ACKNOWLEDGMENTS

I would like to thank Mark Hindmarsh for collaboration on this subject, and Ray Rivers, Erkki Thuneberg and Grisha Volovik for useful discussions. The author was supported by PPARC and also partly by the University of Helsinki. Part of this work was conducted on the SGI Origin platform using COSMOS Consortium facilities, funded by HEFCE, PPARC and SGI.

REFERENCES

1. T. W. Kibble, *J. Phys. A* **9**, 1387 (1976).
2. I. Chuang, R. Durrer, N. Turok and B. Yurke, *Science* **251**, 1336 (1991); M.J. Bowick, L. Chandar, E.A. Schiff and A.M. Srivastava, *Science* **263**, 943 (1994).
3. C. Bäuerle *et al.*, *Nature* **382**, 332 (1996); *J. Low Temp. Phys.* **110**, 13 (1998).
4. V.M.H. Ruutu *et al.*, *Nature* **382**, 334 (1996) [cond-mat/9512117]; V.M.H. Ruutu *et al.*, *Phys. Rev. Lett.* **80**, 1465 (1998) [cond-mat/9706038].
5. M.E. Dodd *et al.*, *Phys. Rev. Lett.* **81**, 3703 (1998).
6. W. H. Zurek, *Phys. Rept.* **276**, 177 (1996) [cond-mat/9607135].
7. R. J. Rivers, E. Kavoussanaki and G. Karra, cond-mat/0001274.
8. R. Carmi and E. Polturak, *Phys. Rev. B* **60**, 7595 (1999) [cond-mat/9908244].
9. R. Carmi, E. Polturak and G. Koren, *Phys. Rev. Lett.* **84**, 4966 (2000).
10. S. Rudaz and A.M. Srivastava, *Mod. Phys. Lett. A* **8**, 1443 (1993) [hep-ph/9212279]; M. Hindmarsh, A. Davis and R. Brandenberger, *Phys. Rev. D* **49**, 1944 (1994) [hep-ph/9307203]; T.W.B. Kibble and A. Vilenkin, *Phys. Rev. D* **52**, 679 (1995) [hep-ph/9501266].
11. M. Hindmarsh and A. Rajantie, *Phys. Rev. Lett.* **85**, 4660 (2000) [cond-mat/0007361].
12. H. Kleinert, *Gauge fields in condensed matter*, (World Scientific, Singapore, 1989).